Proceedings of the ASME 2010 3rd Joint US-European Fluids Engineering Summer Meeting and 8th International Conference on Nanochannels, Microchannels, and Minichannels
FEDSM-ICNMM2010
August 1-5, 2010, Montreal, Canada

FEDSM-ICNMM2010-30545

PERFORMANCE OF A TETHERED POINT WAVE-ENERGY ABSORBER IN REGULAR AND IRREGULAR WAVES

Erin E. Bachynski
Yin Lu Young*
Department of Naval Architecture and Marine Engineering
University of Michigan
Ann Arbor, Michigan, 48019, USA
Emails: ebachyns@gmail.com, ylyoung@umich.edu

Ronald W. Yeung
Department of Mechanical Engineering
University of California at Berkeley
Berkeley, California, 94720, USA
Email: rwyeung@berkeley.edu

ABSTRACT

The importance of the mooring system on the dynamic response of a point-absorber type ocean-wave energy converter (WEC) is investigated using a frequency-domain approach. In order to ensure the safety of WECs, careful consideration of the response and resonance frequencies in all motions must be evaluated, including the effects of the mooring system. In this study, a WEC floater with a closed, flat bottom is modeled as a rigid vertical cylinder tethered by elastic mooring lines. The WEC hydrodynamic added mass and damping are obtained using established potential-flow methods, with additional damping provided by the energy-extraction system. The results show that the response of the WEC, and the corresponding power takeoff, varies with the diameter-to-draft (D/T) ratio, mooring system stiffness, and mass distribution. For a given wave climate in Northern California, near San Francisco, the heave energy extraction is found to be best for a shallow WEC with a soft mooring system, compared to other systems that were examined. This result assumes a physical limit (cap) on the motion which is related to the significant wave height to draft ratio. Shallow draft designs, however, may experience excessive pitch motions and relatively larger viscous damping. In order to mitigate the pitch response, the pitch radius of gyration should be small and the center of mass should be low.

*Correspondence author: ylyoung@umich.edu

NOMENCLATURE

A	Mooring line cross-sectional area
B_{jjPTO}	Power takeoff damping coefficient
C_{ij}	Hydrodynamic restoring force coefficient
D	WEC Diameter ($= 2\times$radius, a)
$\vec{e}_x$	Unit vector in x
$\vec{e}_y$	Unit vector in y
$\vec{e}_z$	Unit vector in z
E	Mooring line Young's modulus
$\widetilde{F}_{ej}$	Complex dimensional wave-exciting force in the j-th direction
ζ_0	Incident wave amplitude
ζ_1	Surge motion amplitude $= \lvert\widetilde{\zeta}_1\rvert$
$\widetilde{\zeta}_1$	Complex surge motion amplitude
ζ_3	Heave motion amplitude $= \lvert\widetilde{\zeta}_3\rvert$
$\widetilde{\zeta}_3$	Complex heave motion amplitude
ζ_5	Pitch motion amplitude $= \lvert\widetilde{\zeta}_5\rvert$
$\widetilde{\zeta}_5$	Complex pitch motion in radians
$\zeta_{j_{exp}}$	Spectral expected motion amplitude of the j-th mode
H	Water depth
H_{P_j}	Power transfer function of j-th mode (in Wm^{-1})
H_{R_j}	Response amplitude operator of j-th mode (m/m or rad/m)
H_s	Significant wave height

I_t	Mooring system moment of inertia about WEC center of flotation
θ_j	Mooring line j attachment angle from the x-axis
J_j	Annual energy extraction for the j-th mode
K_{ij}	Mooring line restoring force coefficient
λ_{ij}	Non-dimensional radiation damping coefficient
$\overline{\lambda}_{ij}$	Dimensional radiation damping coefficient
l	Initial mooring line length
L	Cylinder total height
μ_{ij}	Non-dimensional added mass coefficient
$\overline{\mu}_{ij}$	Dimensional added mass coefficient
M	WEC mass
M_{ij}	Mass matrix coefficient
MS1	Mooring system 1
MS2	Mooring system 2
M_t	Mooring system total mass
n	Number of mooring lines
$P_{j_{exp}}$	Spectral expected power takeoff for the j-th motion mode
P_j	Time-averaged power takeoff for the j-th motion mode
ρ	Water density
$\vec{r}$	Vector from center of flotation to mooring line attachment point
r_p	Radius of gyration for pitch
r_p^*	Non-dimensional radius of gyration for pitch, r_p/T
$S_{P_j}^+$	Power takeoff spectrum of j-th mode in W^2s
$S_{R_j}^+$	Response spectrum of j-th mode (m^2s or rad^{2}s)
$S^+(\omega)$	Wave spectrum
$\vec{t}$	Unit vector along direction of mooring line
T	WEC Draft
T_w	Wave period
T_z	Mean wave period
UM	Unmoored
w	Mooring line mass per unit length
X_j	Non-dimensional wave-exciting force in direction j per unit ζ_0
ω	Incident wave frequency
ω_3	Heave resonance frequency
ω_{51}	Coupled surge-pitch resonance frequency
ω_z	Mean wave frequency
z_G	Vertical coordinate of the center of gravity
z_G^*	Non-dimensional vertical coordinate of the center of gravity, z_G/T

INTRODUCTION

Wave energy converters (WECs) have the technical and economic potential to contribute significantly to the renewable energy mix [1]. While laboratory tests show promise and a variety of devices have been tested and connected to the grid, survivability remains a design challenge, as exemplified by the loss of Finavera's prototype floater off the Oregon coast in November 2007 [2]. Therefore, improved prediction models for the WEC response are necessary. In particular, the effects of the mooring system on the system responses and possible system failure modes are important considerations.

A linear, frequency-based analysis of a tethered cylindrical floater is used to investigate the system resonances and responses. Numerous references on the hydrodynamic characteristics of a vertical surface-piercing cylinder in finite depth water are available. Analytical solutions for the hydrodynamic coefficients and wave forcing based on potential flow formulations and eigenfunction expansions can be found in [3–5]. Validations of numerical predictions following the same methods with experimental measurements for an unmoored surface piercing cylinder in finite depth water can be found in [6]. The simplified situation for shallow water (relative to the cylinder draft) is given by [7].

The frequency-dependent hydrodynamic coefficients and the response of a moored WEC are analyzed in [8, 9]. Eriksson et. al. considered a heaving disk-like cylinder with a linear restoring force and linear damping to represent the power takeoff system [8]. Fitzgerald and Bergdhal considered the surge, heave, and pitch motions of a moored WEC in regular waves, and compared results for an unmoored system with a linearized power takeoff system [9].

The objective of this paper is to evaluate the effects of the floater dimensions, mass distribution, and mooring system on the system responses of WECs in regular and irregular waves, particularly as related to the resonance frequencies. This work provides an extension of previous studies which consider motions limited to a single degree of freedom (DOF) [8], or limited design cases [9] in regular waves. Consideration of the spectral response is important, since the device will operate in a stochastic environment with a range of excitation frequencies. The goal is to be able to optimally tune a tethered WEC for a given probable wave climate to maximize the overall energy extraction while ensuring system structural integrity.

WAVE ENERGY CONVERTER MODEL

Problem setup

The setup for the 3-DOF problem is illustrated in Figure 1. Surge ($\widetilde{\zeta}_1$), heave ($\widetilde{\zeta}_3$), and pitch ($\widetilde{\zeta}_5$), motions, all defined about the center of flotation, are considered. As shown, the cylinder has a diameter D, draft T, and overall length L. The center of gravity CG is necessarily low in order to provide pitch stability. The coordinate system is taken at the center of flotation of the cylinder in still water, with the z axis pointing vertically upward and the x direction aligned with the direction of wave propagation. The incoming waves have amplitude ζ_0, and frequency ω. The water depth is H and n mooring lines are considered.

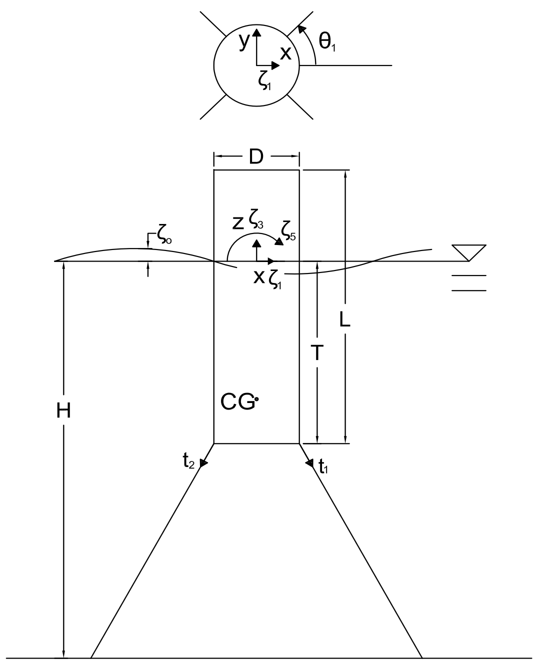

FIGURE 1. WAVE ENERGY CONVERTER MODEL TOP AND SIDE VIEWS.

Geometry

Two possible geometries for the WEC are considered; both have $D = 5$ m while the draft is varied between $T = 10$ m and $T = 20$ m. Interesting hydrodynamic results are noted for cylinders with $D/T \approx 1$ due to the cancellations and interactions between bottom and side forces in the pitch added mass; however, current design trends favor deeper drafts. The displacement and weight are taken to be equal and only stable configurations are considered, so that the dynamics of a freely-floating (untethered) cylinder may be compared. The water depth is held constant at $H = 50$ m, which is a reasonable installation depth [9, 10].

Mass Distribution

Here, the mass (M) of the WEC is dictated by the geometry as in Eqn. (1) in order to match the weight and displacement,

$$M = M_{11} = M_{33} = \frac{\rho \pi T D^2}{4} \tag{1}$$

where M_{ij} are elements of the generalized mass matrix of multiple degrees of freedom of motion (see Eqn. (8)). The mass distribution of the WEC is an important design consideration, particularly when pitch motions are considered. The mass distribution is defined by the vertical location of the center of gravity, z_G, and the radius of gyration, r_p. z_G affects the mass coupling between pitch and surge, while r_p specifies the mass moment of inertia of the WEC per Eqn. (2).

$$M_{15} = M_{51} = M z_G, \quad M_{55} = M {r_p}^2 \tag{2}$$

The design mass distribution of existing WECs is not known a priori. A range of z_G and r_p are considered; however, it should be noted that not all combinations may be practical for construction. For example, achieving a low radius of gyration with the center of gravity close to the keel may not be possible.

Added Mass, Radiation Damping, and Wave Forces

The frequency-dependent added mass ($\overline{\mu}_{ij}$) and damping ($\overline{\lambda}_{ij}$) are found by solving the potential function using an eigenfunction expansion, as in [4]. Validations of the non-dimensional added mass (μ_{ij}), damping (λ_{ij}), and forcing ($|X_j|$) coefficients show excellent agreement with numerical and experimental simulations presented in [4, 8, 11].

Added mass and damping coefficients for the two cylinder geometries are shown in Figs. 2 and 3, where the non-dimensionalizations follow [4]. As shown, the coupled pitch-surge added mass and damping are negative due to the choice of the coordinate systems.

Non-dimensionalized wave force amplitude ($|X_j|$), which can be obtained from the radiation damping of [4] via the use of the Haskind Relation [12], is shown in Fig. 4.The heave forcing per unit wave amplitude tends to increase with period, while the surge and pitch forcing reach a peak and subsequently decrease. The wave forcing phase angle relative to the incident wave is not shown; the complex form of the wave forcing follows [3, 5]. It is important to note that the surge and pitch wave forcing are out of phase. Neglecting the forcing phase would lead to incorrect results for the surge-pitch coupled response.

Mooring Line Restoring Forces and Mass

The mooring system is assumed to be comprised of n linear springs, attached at angle θ_j from the x-axis, with $j = 1, 2, 3...n$, as in Fig. 1. This model assumes linear geometry and small motions. For each line, the spring stiffness is given by K_j, which is a function of the Young's modulus of the line (E_j), the cross-sectional area of the lines (A_j) and the initial length of the lines (l_j), as in Eqn. (3).

$$K_j = E_j A_j / l_j \tag{3}$$

The linearized mooring forces effectively contribute to the restoring force (C) matrix. It should be noted that catenary mooring systems may be represented similarly by computing the slope of the load-deformation responses for the mooring system, which provides the values of the stiffness terms K_{11}, K_{33}, and K_{55}. For

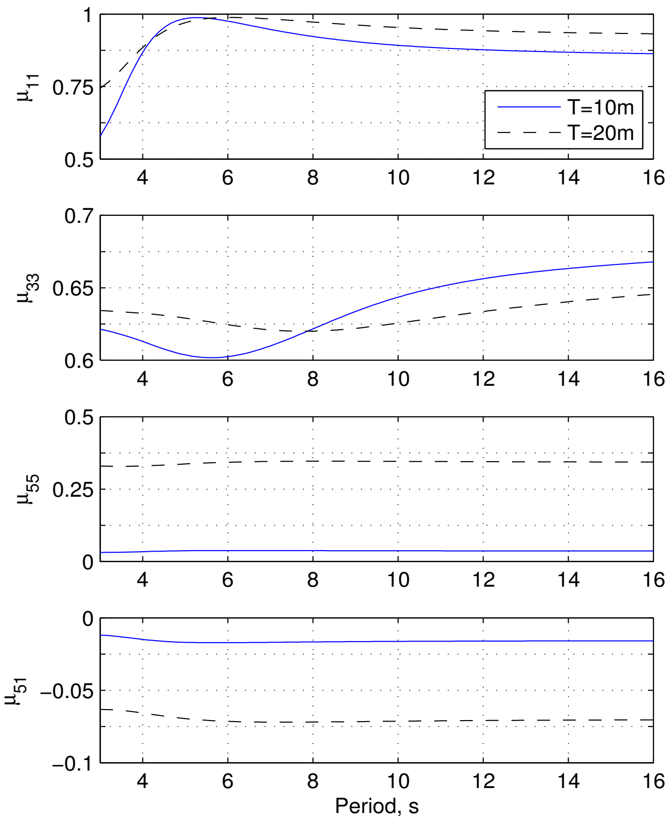

FIGURE 2. NON-DIMENSIONAL ADDED MASS IN SURGE, HEAVE, PITCH, AND COUPLED SURGE-PITCH AS A FUNCTION OF WAVE PERIOD.

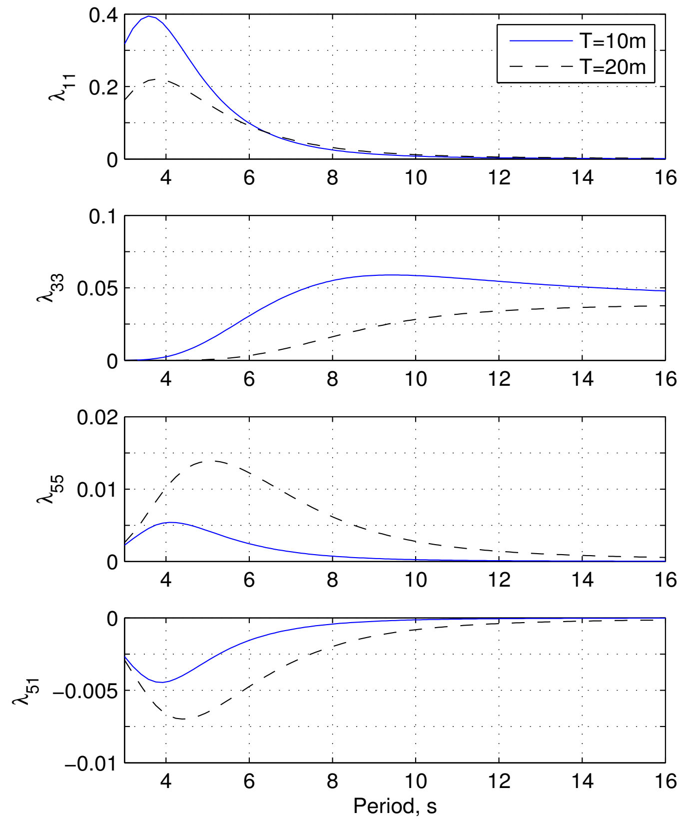

FIGURE 3. NON-DIMENSIONAL DAMPING IN SURGE, HEAVE, PITCH, AND COUPLED SURGE-PITCH AS A FUNCTION OF WAVE PERIOD.

the linear spring model, the stiffness terms due to the mooring lines are given in Eqns. (4)-(6).

$$K_{11} = \sum_{j=1}^{n} K_j |\vec{t}_j \bullet \vec{e}_x| \tag{4}$$

$$K_{33} = \sum_{j=1}^{n} K_j |\vec{t}_j \bullet \vec{e}_z| \tag{5}$$

$$K_{55} = \sum_{j=1}^{n} K_j |(\vec{t}_j \times \vec{r}_j) \bullet \vec{e}_y| \tag{6}$$

where $\vec{e}_x$, $\vec{e}_y$, and $\vec{e}_z$ are unit vectors in the x, y, and z directions. The vector $\vec{r}$ is directed from the center of flotation to the mooring line attachment point on the cylinder, while $\vec{t}$ is directed from the line attachment point on the cylinder to the anchor point on the seabed.

Two specific mooring systems are considered. The first, Mooring System 1 (MS1) is adopted following [9]. The mooring system consists of four catenary chains (EA = 100 MPa, w = 61 kg/m, 34 kN pretension at attachment). The restoring matrix coefficients and mass effects of MS1 are given in Tab. 1, following an approximation to the linearization of [9] for a catenary system with line length 100 m. Here, M_t is the total mass of the mooring system and I_t is the moment of inertia of the mooring system about the center of flotation. The mooring system also contributes to the coupled mass coefficient M_{51}, which is found by multiplying T and M_t. As shown, the mooring system mass represents approximately 8.5 percent of the WEC mass for the $T = 10$ m model. The draft of the floater increases in order to accommodate the increased mass.

The second mooring system consists of four synthetic tethers with stiffness $EA = 1$ MPa and mass $w = 8.6$ kg/m, attached at inclination angles of 40 degrees. The restoring matrix coefficients and mass effects for Mooring System 2 (MS2) are given in Tab. 2. Here, the stiffness terms follow the same linear spring model and the pretension is 16 kN.

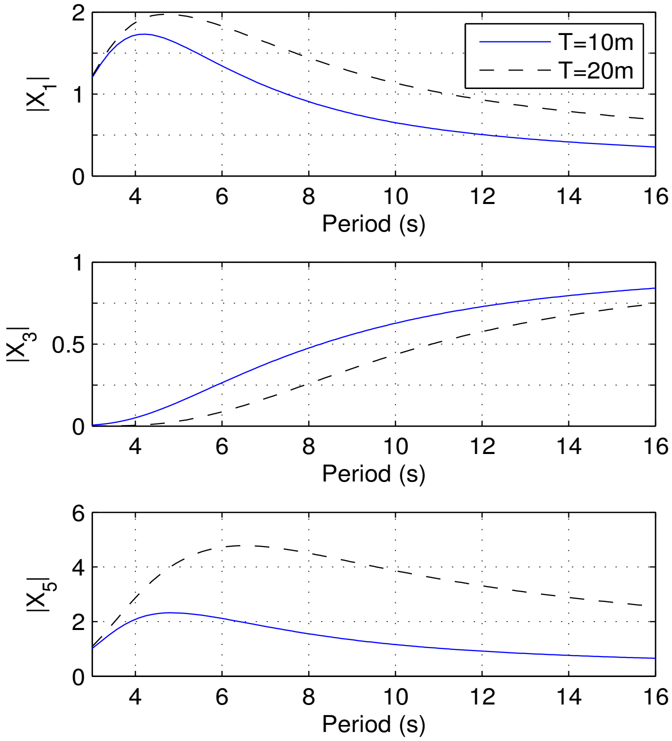

FIGURE 4. NON-DIMENSIONAL WAVE EXCITING FORCE AMPLITUDES PER UNIT WAVE AMPLITUDE AS A FUNCTION OF WAVE PERIOD.

TABLE 1. MOORING SYSTEM 1 CHARACTERISTICS

	T=10m	T=20m
K_{11} (kN/m)	4.0	4.0
K_{33} (kN/m)	6.0	6.0
K_{55} (kNm/rad)	140.0	280.0
M_t (kg)	1.71x10^4	1.46x10^4
M (kg)	2.01x10^5	4.02x10^5
I_t (kgm^2)	1.76x10^6	5.85x10^6

Power Takeoff System

The power takeoff system is assumed to contribute a linear damping term in heave and pitch ($B_{jj_{PTO}}, j = 3,5$). The time averaged absorbed power (P_j) is found from Eqn. (7), as in [9], where $\dot{\zeta}_j$ is the velocity amplitude:

$$P_j(\omega) = \frac{B_{jj_{PTO}}(\dot{\zeta}_j(\omega))^2}{2}, j = 3,5 \tag{7}$$

TABLE 2. MOORING SYSTEM 2 CHARACTERISTICS

	T=10m	T=20m
K_{11} (kN/m)	24.6	32.8
K_{33} (kN/m)	58.7	78.2
K_{55} (kNm/rad)	172.8	558.7
M_t (kg)	1.80x10^3	1.35x10^3
M (kg)	2.01x10^5	4.02x10^5
I_t (kgm^2)	1.85x10^5	5.43x10^5

The optimal power takeoff system damping, as shown in [13], is equal to the total hydrodynamic damping at resonance for each particular system configuration. In this case, as opposed to [13], viscous damping is ignored, so the optimal power takeoff damping is equal to the wave radiation (potential) damping, which is known to lead to excessive motion. The value of $B_{33_{PTO}}$ varies significantly with draft for the different mooring systems, as shown in Fig. 5. As our intention is to assess merely the extent of the surge and pitch motion, in this work, $B_{55_{PTO}}$ is taken to be zero, although designs which rely upon pitch motions do exist. No power takeoff in surge is considered, though such a system is also possible.

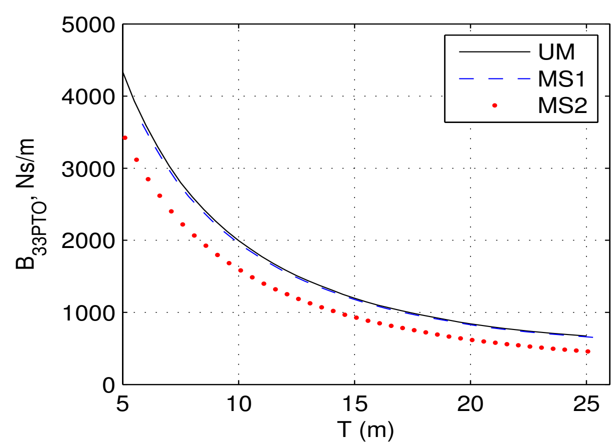

FIGURE 5. HEAVE POWER TAKEOFF DAMPING FOR VARYING DRAFT.

Frequency Domain Equations of Motion

The equations of motion, Eqn. (8), are formulated and solved in the frequency domain using an original MATLAB code. The hydrostatic restoring force coefficients (C_{33} and C_{55})

are functions of the waterplane area and the location of the center of gravity, as in Eqn. (9) and Eqn. (10). For the two considered floaters, the hydrostatic restoring force coefficients are given in Tab. 3.

$$
\begin{aligned}
&-\omega^2 \begin{bmatrix} M_{11}+\overline{\mu}_{11}+M_t & 0 & M_{15}+\overline{\mu}_{15}-TM_t \\ 0 & M_{33}+\overline{\mu}_{33}+M_t & 0 \\ M_{51}+\overline{\mu}_{51}-TM_t & 0 & M_{55}+\overline{\mu}_{55}+I_t \end{bmatrix} \begin{bmatrix} \widetilde{\zeta}_1 \\ \widetilde{\zeta}_3 \\ \widetilde{\zeta}_5 \end{bmatrix} \\
&+i\omega \begin{bmatrix} \overline{\lambda}_{11} & 0 & \overline{\lambda}_{15} \\ 0 & \overline{\lambda}_{33}+B_{33_{PTO}} & 0 \\ \overline{\lambda}_{51} & 0 & \overline{\lambda}_{55}+B_{55_{PTO}} \end{bmatrix} \begin{bmatrix} \widetilde{\zeta}_1 \\ \widetilde{\zeta}_3 \\ \widetilde{\zeta}_5 \end{bmatrix} \\
&+ \begin{bmatrix} K_{11} & 0 & 0 \\ 0 & C_{33}+K_{33} & 0 \\ 0 & 0 & C_{55}+K_{55} \end{bmatrix} \begin{bmatrix} \widetilde{\zeta}_1 \\ \widetilde{\zeta}_3 \\ \widetilde{\zeta}_5 \end{bmatrix} = \begin{bmatrix} \widetilde{F}_{e1} \\ \widetilde{F}_{e3} \\ \widetilde{F}_{e5} \end{bmatrix}
\end{aligned} \tag{8}
$$

$$
C_{33} = \rho g \pi \frac{D^2}{4} \tag{9}
$$

$$
C_{55} = Mg\left(\frac{D^2}{16T} + T/2 - (z_G + T)\right) \tag{10}
$$

The system [8] shows that the heave motion is decoupled hydrodynamically from the surge and pitch modes because of the symmetric arrangement of the mooring lines and the linearization procedure. As mentioned earlier, the phasing of $\tilde{F_{e1}}$ (or X_1) and $\tilde{F_{e5}}$ (or X_5) are important in determining the surge-pitch coupled motions. It is of interest to know the expected behavior of $\tilde{F_{e1}}$ and $\tilde{F_{e5}}$ as this aspect was not clearly discussed in [3]. It is relatively straight-forward to establish that in deep water, and in the low-frequency (or long-wave) limit, these forces can be given analytically by [14]:

$$
\tilde{F_{e1}} = -\zeta_o\left[\frac{\pi\rho g D T}{2} + \frac{2g}{D}(\bar{\mu}_{11} + i\bar{\lambda}_{11})\right] ka + O((ka)^2) \tag{11}
$$

$$
\tilde{F_{e5}} = \zeta_o\left[\frac{\pi\rho g D}{2}(T^2 - \frac{D^2}{16}) - \frac{2g}{D}(\bar{\mu}_{15} + i\bar{\lambda}_{15})\right] ka + O((ka)^2) \tag{12}
$$

Equations (11)-(12) contain both Froude-Krylov and diffraction effects. Given that the damping $\bar{\lambda}'s$ are vanishingly small, we note that the surge force is 180^o out of phase with the wave slope $k\zeta_o$, an expected physical behavior, while the pitch moment, for a deeper cylinder ($T > D/4$), is definitely in phase with the wave slope because of the negativeness of $\bar{\mu}_{15}$ and $\bar{\lambda}_{15}$ for our T/D proportions. However, a shallower draft cylinder may change the phase property of the pitch moment. The force and moment amplitudes based on these analytical results are consistent with [4, 6], as $ka \to 0$, while the phases are consistent consistent with [11] for the open-water case shown therein and [5]'s reproduction of [3].

TABLE 3. HYDROSTATIC RESTORING FORCE COEFFICIENTS

	T=10m	T=20m
C_{33} (kN/m)	197.4	197.4
$C_{55}+Mg(z_G+T)$ (MNm/rad)	10.1	39.7

Expected Resonance Frequencies (Freely Floating WEC)

A freely floating cylinder experiences resonance for two frequencies, ω_3 and ω_{51}. The resonance frequency in heave (ω_3) is obtained from the decoupled single degree of freedom model as in Eqn. (13), where the added mass $\overline{\mu}_{33}$ is evaluated at the resonance frequency for the particular system configuration. Variations in the added mass may theoretically result in multiple resonance frequencies; however, such effects can only be correctly captured using nonlinear methods.

$$
\omega_3 = \sqrt{\frac{C_{33}}{(M_{33} + \overline{\mu}_{33})}} \tag{13}
$$

The coupled surge-pitch resonance frequency, ω_{51} is given by Eqn. (14). For a freely floating cylinder, a single resonance frequency for the coupled motion is expected, since there is no stiffness in surge. In certain cases (when the denominator is less than zero), there may be not be any real solutions to Eqn. (14).

$$
\omega_{51} = \sqrt{\frac{C_{55}(M_{11} + \overline{\mu}_{11})}{(M_{11} + \overline{\mu}_{11})(M_{55} + \overline{\mu}_{55}) - (M_{51} + \overline{\mu}_{51})^2}} \tag{14}
$$

We note that the sign of $\overline{\mu}_{51}$ has critical effect.

Expected Resonance Frequencies (Moored WEC)

For a moored cylinder, the resonance frequency for the decoupled heave motion is given by Eqn. (15). For the linear spring model (MS2), the increase in stiffness provided by the mooring system results in a higher resonance frequency compared to the unmoored case, since the increase in mass is found to be a smaller effect. For the catenary chain (MS1) the mass effects are more significant than the stiffness effects and the resonance frequency decreases.

$$
\omega_3 = \sqrt{\frac{C_{33} + K_{33}}{(M_{33} + \overline{\mu}_{33} + M_t)}} \tag{15}
$$

The coupled surge-pitch resonances occur at two distinct frequencies of ω_{51}. These can be found by solving for the real roots of Equation (16).

$$\omega_{51}{}^4\left((M_{11}+\overline{\mu}_{11}+M_t)(M_{55}+\overline{\mu}_{55}+I_t)-(M_{51}+\overline{\mu}_{51}-TM_t)^2\right)+$$
$$\omega_{51}{}^2\left(-(C_{55}+K_{55})(M_{11}+\overline{\mu}_{11}+M_t)-K_{11}(M_{55}+\overline{\mu}_{55}+I_t)\right)$$
$$+K_{11}(C_{55}+K_{55})=0 \tag{16}$$

Response amplitude operators (RAOs)

The frequency-dependent response (for unit-amplitude waves), or RAO, is defined as in Eqn. (17).

$$H_{R_j}=\frac{|\widetilde{\zeta}_j|}{\zeta_0}, j=1,3,5 \tag{17}$$

As shown in Fig. 6, the heave RAO is limited to $H_{R_3}\leq T/(2H_s)$, where H_s is the significant wave height, to account for viscous effects and prevent excessive motions. MS1 shows a slightly longer resonance period because the increase in mass has a greater effect than the increase in stiffness; MS2 shows a shorter resonance period because the increase in stiffness has a greater effect than the increase in mass. As the draft increases, the heave resonance period increases due to the increased mass.

Surge and pitch RAOs for several mass distributions are shown in Fig. 7. For the unmoored (UM) WEC, a pitch resonance response is seen at wave period T_w = 6.5 seconds for the highest radius of gyration with a relatively high center of gravity (r_p/T = 0.8 and z_G/T = -0.7). The pitch motion is limited to 30 degrees per meter of wave amplitude, surge is capped at 5 times the wave amplitude. The unmoored WEC does not show resonant response for certain mass distributions since there are no real roots from Eqn. (14).

The addition of MS1 results in a longer resonance period (6.7 seconds) in pitch for r_p/T = 0.8 and z_G/T = -0.7. Furthermore, resonant responses are seen for all cases for MS1 for very long periods, which are unlikely to be excited. For the stiffer system (MS2), there is a resonance at 5.9 seconds as well as a long period resonance around 24 seconds, which may be excited by long swells.

SPECTRAL RESPONSE IN A WAVE ENVIRONMENT

Northern California wave climate

Wave data from 2005-2009 from the National Data Buoy Center Buoy 46026 [15], located at 37.759N 122.833W, were analyzed as a representative wave climate for energy harvesting. The mean winter and summer wave climates are shown in Fig. 8. As shown, fitted ISSC spectra are used to represent these seasonal trends. The ISSC spectrum is a standard two-parameter

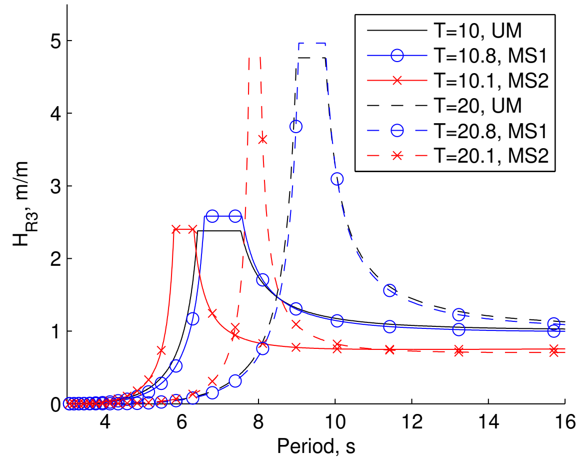

FIGURE 6. HEAVE RAOS (CAP BASED ON WINTER WAVE CLIMATE AT NDBC BUOY 46026, NORTHERN CALIFORNIA).

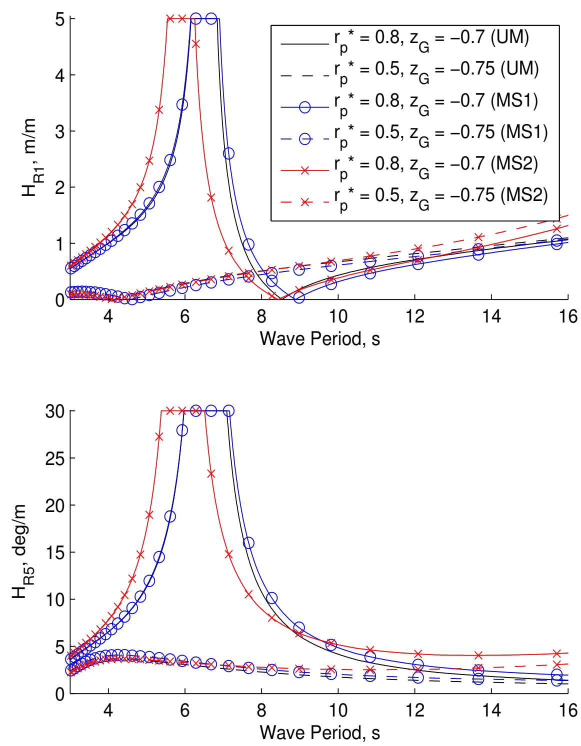

FIGURE 7. SURGE AND PITCH RAOS ($T=10$ m).

spectrum, as defined in Eqn. (18), which is taken from [16]:

$$S^+(\omega)=0.11{H_s}^2\frac{{\omega_z}^4}{\omega^5}\exp\left(-0.44\left(\frac{\omega_z}{\omega}\right)^4\right) \tag{18}$$

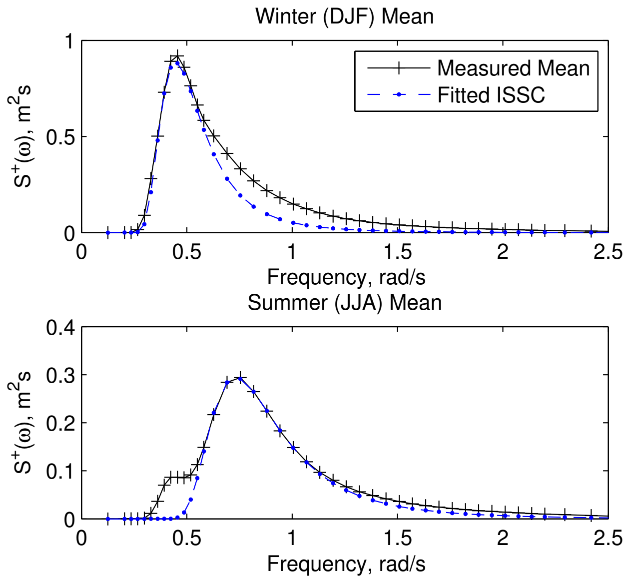

FIGURE 8. WINTER AND SUMMER WAVE CLIMATE (NDBC BUOY 46026, NORTHERN CALIFORNIA).

where ω_z is the mean frequency ($\omega_z = 2\pi/T_z$) and H_s is the significant wave height. The winter wave climate is represented with ω_z = 0.58 rad/s and H_s = 2.10 m; the summer has ω_z = 0.95 rad/s and H_s = 1.55 m. Note that this approximation of the wave climate using the ISSC spectrum neglects low frequency energy in summer. Caution should be employed when using fitted spectra: resonant response, particularly in pitch, maybe be missed using this approximation.

Spectral Response

The spectral response of the WEC (S_R^+) is a function of the wave input spectrum and the RAO as in Eqn. (19):

$$S_{R_j}^+(\omega) = [\mathrm{H}_{R_j}(\omega)]^2 S^+(\omega) \tag{19}$$

Similarly, the power takeoff can be analyzed for a given wave spectrum. The spectral power takeoff is:

$$S_{P_j}^+(\omega) = [\mathrm{H}_{P_j}(\omega)]^2 S^+(\omega) \tag{20}$$

where

$$\mathrm{H}_{P_j} = \frac{P_j}{\zeta_0}, j = 1,3,5 \tag{21}$$

and P_j is as defined in Eqn. (7). The expected power ($P_{j_{exp}}$) is then computed as the square root of the area under the power takeoff curve (Eqn. 22).

$$P_{j_{exp}} = \sqrt{\int_0^\infty S_{P_J}^+(\omega) d\omega} \tag{22}$$

The expected amplitude ($\zeta_{j_{exp}}$) for a particular motion can also be found, as in Eqn. (23).

$$\zeta_{j_{exp}} = \sqrt{\int_0^\infty S_{R_j}^+(\omega) d\omega}, j = 1,3,5 \tag{23}$$

Heave Energy Extraction

The heave response of moored and unmoored cylinders is decoupled from the pitch and surge responses. The heave energy extracted over a year (J_3) is used to compare the designs; J_3 is computed from the expected heave power in winter and summer, assuming each season to last approximately 182 days. Table 4 shows the seasonal expected power and the annual energy extraction for each design. These values give a qualitative comparison between the systems, rather than a quantitative analysis, because of the absence of viscous effects, the use of a linear analysis, and the implementation of an arbitrary motion cap. Although the winter wave heights are larger, the summer power extraction is greater due to the higher frequency motions and the closer correspondence between the excitation and resonance frequencies. However, a change in draft by reballasting can provide equally favorable energy yield.

In this analysis, the motion cap is reached by all designs, such that the largest power extraction occurs for higher resonance frequencies (corresponding to higher velocity at resonance) and higher values of $B_{33_{PTO}}$. Shallower draft designs are preferred according to this measure; however, these designs may suffer from excessive pitch motions and relatively larger viscous damping. For extremely shallow drafts, the heave motion is limited by the floater dimensions and the power takeoff decreases. Furthermore, the softer mooring system is clearly preferable to the stiff mooring system. Real WEC designs should be better tuned to the particular wave climate and utilize higher power takeoff damping values.

Surge and Pitch Response

In general, the energy extraction system is expected to take advantage of heave motion; however, certain systems may also be able to extract energy from surge and/or pitch motions. Two types of designs are considered: those that desire to mitigate pitch in order to increase the system stability and lifespan and those that seek to extract energy from the pitch motions. The expected pitch response for the freely floating WEC is shown as a function of r_p/T and z_G/T in Figs. 9 and 10 for the winter and summer, respectively. The pitch response is maximized for different ranges of mass distributions in both cases; the response tends to be greater in the summer due to the wider range of excitation frequencies. If pitch power can be extracted, the year-round optimum must be considered. On the other hand, in order to minimize the pitch response, designers should look to

TABLE 4. ANNUAL HEAVE ENERGY EXTRACTION FOR A WEC LOCATED NEAR NDBC BUOY 46026, NORTHERN CALIFORNIA.

	Winter $P_{3_{exp}}$ (kW)	Summer $P_{3_{exp}}$ (kW)	J_3 (GJ)
$T = 10$m			
UM	0.63	1.46	32.86
MS1	0.60	1.40	31.39
MS2	0.37	0.97	21.12
$T = 20$m			
UM	0.66	0.95	25.27
MS1	0.64	0.91	24.31
MS2	0.36	0.74	17.20

minimize the radius of gyration and keep a low center of gravity, which may be conflicting requirements. An important design consideration for WECs may be the steep pitch response gradient with respect to the mass distribution for designs with high r_p.

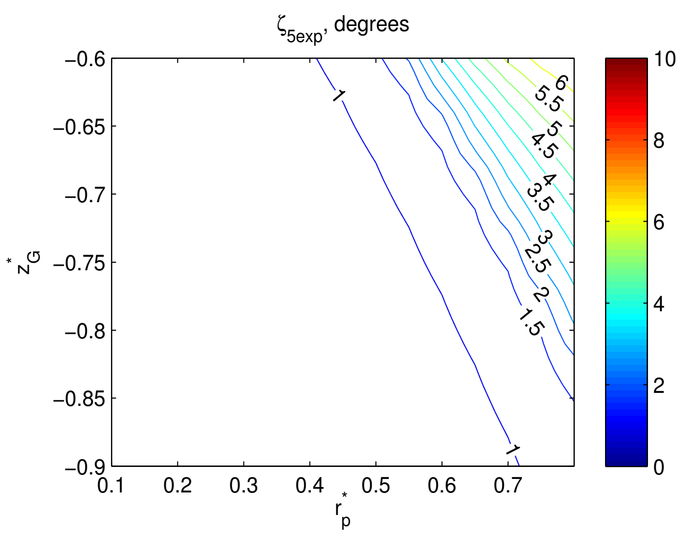

FIGURE 9. EXPECTED PITCH RESPONSE (DEGREES) IN WINTER $T = 10$ m, UM.

The expected pitch response for MS1 in the winter is shown in Fig. 11. The soft mooring system causes a small increase in the pitch motion response compared to the UM case (Fig. 9), since the resonance frequency is not significantly modified by the mooring lines. Nevertheless, the addition of the mooring system imposes a restriction on the optimal r_p^* and z_G^* if the pitch response were to be minimized.

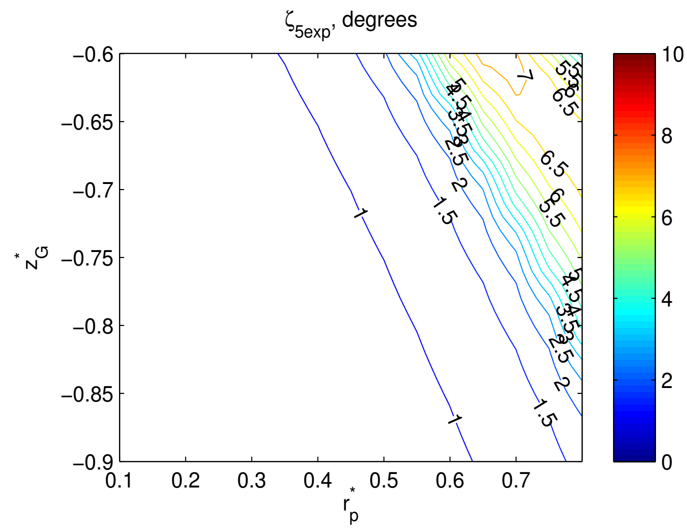

FIGURE 10. EXPECTED PITCH RESPONSE (DEGREES) IN SUMMER, $T = 10$ m, UM.

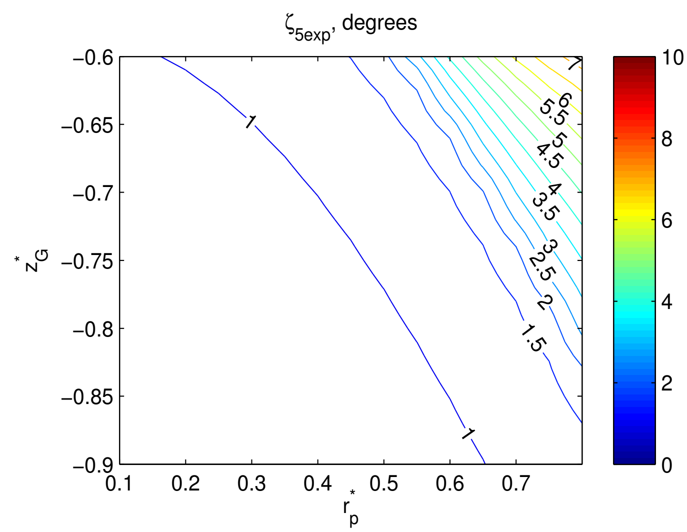

FIGURE 11. EXPECTED PITCH RESPONSE (DEGREES) IN WINTER, $T = 10$ m, MS1.

The expected pitch response for MS2 in the winter is shown in Fig. 12. In general, the stiffer mooring system results in larger pitch response, and hence will impose an even more stringent restriction on r_p^* and z_G^* if the pitch response is to be minimized. For the stiffer system, it should be noted that sea spectra for storm and swell conditions may also result in changes in the response trends related to the mass distribution due to excitation of the lower resonance frequency.

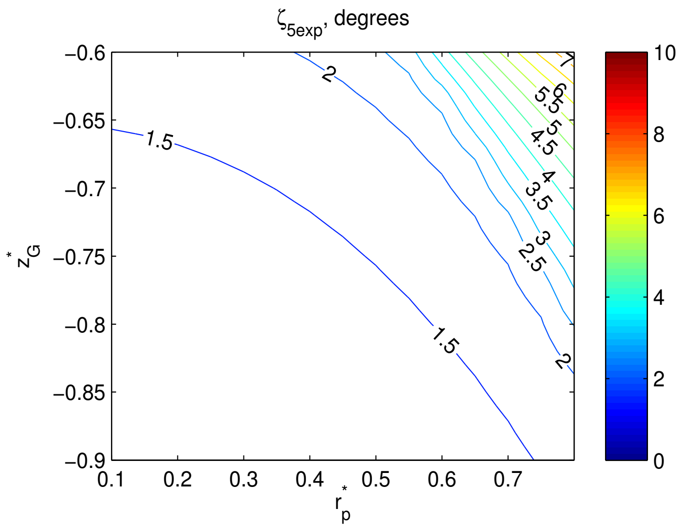

FIGURE 12. EXPECTED PITCH RESPONSE (DEGREES) IN WINTER, $T = 10$ m, MS2.

CONCLUSIONS

Both the mooring system and the mass distribution contribute to variations in the resonance frequencies of a WEC. In order to efficiently capture energy over a range of sea conditions, while avoiding failure modes due to excessive motions, careful consideration of the system resonances and wave-excitation frequencies is necessary. The mooring system significantly impacts the energy capture. Pitch and surge response are heavily influenced by the system mass distribution and the mooring configuration, therefore, design of the WEC should include analysis of the possible pitch mitigation for heave-type devices in the dominant or storm sea states through optimization of the mass distribution with consideration for the mooring system. The focus of the present work is on the WEC dynamics and the level of mechanical power achievable. The actual conversion process from mechanical power to electricity, which is not addressed here, remains a design challenge.

ACKNOWLEDGEMENT

The authors gratefully acknowledge the funding provided by King Abdullah University of Science and Technology (KAUST) to UC Berkeley, under AEA Award # KAUST-25478-EE08K1. The first author would also like to acknowledge the funding provided by the University of Michigan College of Engineering J. Reid and Polly Anderson Fellowship and a SNAME William M. Kennedy Scholarship.

REFERENCES

[1] Bedard, R., McGinnis, D., and Klure, J., 2005. Ocean wave energy conversion technology. Tech. rep., Electric Power Research Institute (EPRI).

[2] Blackwell, R., 2007. "Jostled by wave power, a B.C. firm hopes for calm". *The Globe and Mail*, 18 Dec., p. B3.

[3] Garrett, C. J. R., 1971. "Wave forces on a circular dock". *Journal of Fluid Mechanics,* ***46***(1), pp. 129–139.

[4] Yeung, R. W., 1981. "Added mass and damping of a cylinder in finite-depth waters". *Applied Ocean Research,* ***3***(3), pp. 119–133.[1]

[5] Johansson, M., 1986. Transient motions of large floating structures. Tech. Rep. A:14, Department of Hydraulics, Chalmers University of Technology.

[6] Yeung, R. W. and Sphaier, S. H., 1989. "Wave-interference effects on a truncated cylinder in a channel". *Journal of Engineering Mathematics,* ***23***, pp. 95–117.

[7] Drobyshevski, Y., 2004. "Hydrodynamic coefficients of a floating, truncated vertical cylinder in shallow water". *Ocean Engineering,* ***31***, pp. 269–304.

[8] Eriksson, M., Isberg, J., and Leijon, M., 2005. "Hydrodynamic modelling of a direct drive wave energy converter". *International Journal of Engineering Science,* ***43***, pp. 1377–1387.

[9] Fitzgerald, J. and Bergdahl, L., 2008. "Including moorings in the assessment of a generic offshore wave energy converter: A frequency domain approach". *Marine Structures,* ***21***, pp. 23–46.

[10] Johanning, L., Smith, G. H., and Wolfram, J., 2007. "Measurements of static and dynamic mooring line damping and their importance for floating WEC devices". *Ocean Engineering,* ***34***, pp. 1918–1934.

[11] Yeung, R. W. and Sphaier, S. H., 1989. "Wave-interference effects on a floating body in a towing tank". In Proceedings of the Fourth International Symposium on Practical Design of Ships and Mobile Units (PRADS '89), Vol. 3, pp. 95:1–13.

[12] Wehausen, J. V., 1971. "Motion of floating bodies". *Annual Review of Fluid Mechanics,* ***3***, pp. 231–268.

[13] Yeung, R. W., Peiffer, A., Tom, N., and Matlak, T., 2010. "Design, analysis, and evaluation of the UC-Berkeley wave-energy extractor". In Proceedings of the 29th International Conference on Ocean, Offshore, and Arctic Engineering, Paper no. OMAE2010-20492.

[14] Cochet, C., 2010. "Configuration design and dynamic analysis of a two-component wave-energy absorber". Master's thesis, Department of Mechanical Engineering, University of California at Berkeley.

[15] National Data Buoy Center, 2010. Historical data. Tech. rep., National Oceanic Atmospheric Administration.

[16] Lewis, E., 2003. *Principles of Naval Architecture*. Society of Naval Architects and Marine Engineers.

[1] Errata of this article were published in *Applied Ocean Research, 1982,* ***4***(1), p. 63. Readers should also be aware of that in the upper expression of Eqn. (61) of [4], the term $-sinh(m_o d)/(m_o d)$ should read "+" instead of "−".